atmosphere

MDPI

Article

Long-Term Links Between Precipitation Regimes and $PM_{2.5}$ in an Urban Area of Eastern Amazonia (Belém, Brazil), 1980–2024

Rafael Palácios [1,*], Andrea Machado [1], Rita de Cássia Franco [1], Fernando G. Morais [2,*], Marco A. Franco [3,*], Francisco Oliveira [1], Glauber Cirino [1], Breno Imbiriba [1], João de Athaydes Silva, Júnior [1], Leone F. A. Curado [4], Thiago R. Rodrigues [5], Amaury de Souza [5], João Basso [4], Marcelo Biudes [4], Maurício Moura [1], Julia Cohen [1] and Danielle Nassarden [6]

[1] Institute of Geosciences, Federal University of Pará, UFPA, Belém 66075-110, PA, Brazil; andreapereiramachado34@gmail.com (A.M.); ritafrancodende@gmail.com (R.d.C.F.); franciscogeof@gmail.com (F.O.); glaubercirino@ufpa.br (G.C.); breno.imbiriba@gmail.com (B.I.); athaydes@ufpa.br (J.d.A.S.J.); mauriciomoura@ufpa.br (M.M.); jcpcohen@ufpa.br (J.C.)
[2] Environmental Science and Technologies Department, Brookhaven National Laboratory, New York, NY 11973, USA
[3] Institute of Astronomy, Geophysics and Atmospheric Sciences, University of São Paulo, São Paulo 05508-090, SP, Brazil
[4] Institute of Physics, Federal University of Mato Grosso, Cuiabá 78060-900, MT, Brazil; leone.curado@fisica.ufmt.br (L.F.A.C.); jbassofisico@gmail.com (J.B.); marcelo@fisica.ufmt.br (M.B.)
[5] Institute of Physics, Federal University of Mato Grosso do Sul, Campo Grande 79070-900, MS, Brazil; thiago.r.rodrigues@ufms.br (T.R.R.); amaury.souza@ufms.br (A.d.S.)
[6] State Secretary of Education of the State of Pará, Belém 66820-000, PA, Brazil; dany.nassarden93@gmail.com
* Correspondence: rpalacios@ufpa.br (R.P.); fmorais@bnl.gov (F.G.M.); marco.franco@usp.br (M.A.F.)

Abstract

Air pollution remains a major global environmental risk, and exposure to fine particulate matter ($PM_{2.5}$) is associated with adverse health outcomes even at low concentrations. Meteorological conditions influence $PM_{2.5}$ variability, and precipitation is often expected to reduce particle loads through wet removal. However, humid and wet conditions may coincide with elevated $PM_{2.5}$ under specific atmospheric and compositional conditions. Here, we investigate long-term relationships between precipitation regimes and $PM_{2.5}$ concentrations in the Metropolitan Region of Belém (Eastern Amazonia) over the period 1980–2024. We combined $PM_{2.5}$ from the MERRA-2 reanalysis (including a bias-corrected product) with in situ precipitation records, and classified precipitation conditions using the Standardized Precipitation Index (SPI). We find statistically significant positive long-term tendencies in both precipitation and $PM_{2.5}$. Stratified analyses show that $PM_{2.5}$ concentrations are significantly higher under wet conditions, with a weak but significant positive relationship between SPI and $PM_{2.5}$ ($r = 0.23$ for the full period; $r = 0.24$ for the wet class, p-value < 0.01). These findings indicate that increased precipitation in a strong humid tropical urban environment does not necessarily lead to improved air quality. Instead, wet conditions may favor processes such as hygroscopic growth and secondary aerosol formation, contributing to higher $PM_{2.5}$ concentrations on a monthly scale. Overall, this study highlights the importance of considering precipitation regimes and associated atmospheric processes when assessing air quality in tropical urban environments.

Keywords: standardized precipitation index (SPI); MERRA-2 reanalysis; bias correction; long-range aerosol transport; wet removal

Academic Editor: Pavel Kishcha

Received: 13 March 2026
Revised: 10 April 2026
Accepted: 13 April 2026
Published: 16 April 2026

1. Introduction

Air pollution directly impacts various regions of the world, leading to discussions among global leaders about scientific and political initiatives to address this issue [1]. This is because emissions of gases and particles into the atmosphere have strongly impacted population health [2]. It is estimated that virtually the entire world population is exposed to risks caused by air pollution, resulting in approximately seven million premature deaths per year [3]. The component of air pollution known as particulate matter (PM), specifically fine particulate matter (PM with average diameters $\leq$ 2.5 µm, $PM_{2.5}$), is directly associated with harmful impacts on the respiratory and cardiovascular systems. Vos et al. [2] estimated that in 2019, exposure to $PM_{2.5}$ caused approximately 4 million premature deaths, representing 7.3% of total global mortality that year. Furthermore, there is evidence that even in regions of low exposure, the effects of these particles on population health can be lethal [4]. Beyond emission sources, meteorological conditions modulate $PM_{2.5}$ concentrations and exposure, motivating long-term analyses that link climate variability to air quality.

Brazil has continental dimensions and releases PM emissions from diverse sources of into the atmosphere, varying regionally and locally among urban traffic, industrial activities, vehicular emissions, and biomass burning [5–9]. However, in general, there is still a lack of coverage for air quality monitoring, especially over the northern region of the country [9,10]. This difficulty is partially overcome using satellite products and reanalysis. Satellite-derived $PM_{2.5}$ products estimated by reanalysis models have the advantage of overcoming the limitations of monitoring stations, providing broad spatial and temporal coverage in areas where direct measurements are not possible [2,7,9,11–14]. Nevertheless, $PM_{2.5}$ reanalysis remains challenging due to its relatively coarse spatial resolution, uncertainties in the satellite measurements used as input, and difficulties in representing the relationship between atmospheric column observations and near-surface concentrations [15].

Globally, two reanalysis products have stood out for air quality analysis: the Copernicus Atmosphere Monitoring Service (CAMS) [16,17] and the Modern-Era Retrospective Analysis and Research and Application, version 2 (MERRA-2) [18,19]. In a local assessment in the southern Amazon basin, Nassarden et al. [9] reported better error and overestimation metrics for $PM_{2.5}$ estimation using MERRA-2. MERRA-2 reanalysis products provide aerosol components, optical properties such as aerosol optical depth (AOD), and meteorological variables suitable for deriving $PM_{2.5}$, as they are based on a comprehensive representation of the aerosol lifecycle using robust numerical modeling frameworks. The data are freely available from 1980 to the present and allow for the evaluation of longer time series, contributing to the identification of trends, seasonal patterns, and statistical relationships between meteorological variables and $PM_{2.5}$ [20].

The spatial and temporal variability of $PM_{2.5}$ is influenced by meteorological factors, human activities, and environmental characteristics, which at the microscale are strongly associated with land use and land cover [21,22]. At broader scales, $PM_{2.5}$ is highly affected by meteorological factors, especially precipitation, which contributes to particle removal through wet scavenging. Wet scavenging comprises in-cloud (rainout) and below-cloud (washout) processes, whereby particles are incorporated into cloud droplets or captured by falling hydrometeors and subsequently removed from the atmosphere via deposition [23]. At the same time, wet-season conditions and high near-surface moisture can favor hygroscopic growth of particles and enhance secondary aerosol formation, which may increase PM mass concentrations in aggregated metrics [24]. Therefore, precipitation–PM relationships reflect interacting processes and may not be regulated solely by precipitation intensity, but also by particle size, optical/spectral behavior, and chemical composition [23]. Importantly, the sign and magnitude of precipitation–$PM_{2.5}$ associations can differ between

event scales, when individual rainfall episodes often reduce concentrations via scavenging, and monthly or regime-scale aggregates, which integrate co-varying humidity, atmospheric stability, transport, and emission patterns.

Eastern Amazonia, in northern Brazil, especially the Metropolitan Region of Belém (MRB), is characterized by high rainfall levels throughout the year, with distinct periods of greater and lesser rainfall intensity [25,26]. This hydrological dynamic, associated with accelerated urban growth and anthropogenic emissions, makes the region a strategic environment for investigating precipitation–$PM_{2.5}$ associations. Despite its relevance, investigations integrating rainfall variability and air quality remain scarce in this region. Although the role of precipitation in pollutant removal is well-recognized, gaps persist regarding the behavior of particles in Amazonian urban areas, where local factors such as traffic, industrial activities, and specific meteorological characteristics can generate patterns distinct from those observed in other tropical regions.

In this context, this study aimed to evaluate the association between precipitation regimes and $PM_{2.5}$ concentrations in an urban area of Eastern Amazonia, specifically in the MRB. $PM_{2.5}$ data were separated into different precipitation classes using the Standardized Precipitation Index (SPI), enabling regime-scale comparisons based on monthly and long-term aggregates. This analysis used $PM_{2.5}$ estimates from MERRA-2 between 1980 and 2024, and evaluated trends in time series of precipitation, air quality index, and $PM_{2.5}$.

2. Materials and Methods

2.1. Study Area and Precipitation Data

The study was conducted in the Metropolitan Region of Belém, Pará State (MRB), Eastern Amazonia, northern Brazil (Figure 1). Belém, the state capital, has a total area of 1059 km^2, an estimated population of approximately 1.4 million inhabitants, and a population density of 1230 inhabitants km^{-2} [27]. When disregarding the extensive hydrographic portion of the municipality and considering the main inhabited land areas, including smaller islands to the south and larger islands to the north, the land area is approximately 509 km^2. In addition to Belém, the MRB comprises seven neighboring municipalities: Ananindeua, Marituba, Benevides, Santa Bárbara do Pará, Santa Izabel do Pará, Castanhal, and Barcarena, totaling an approximate population of 2.3 million inhabitants [27].

The regional climate is characterized by two main periods: a wet season (January to April) and a dry or less wet season (July to November), with December, May, and June representing transition months between these periods [26]. In climatological terms, the first four months of the year are typically associated with higher rainfall and slightly lower mean air temperatures (below 26.6 °C), whereas the second half of the year tends to present lower rainfall and higher mean air temperatures (above 27 °C) [25]. The MRB is classified as a humid tropical climate (Am) according to the Köppen system, with high temperatures and humidity throughout the year, high rainfall totals, and a strong influence of the Intertropical Convergence Zone (ITCZ) and local convection [26,28].

For precipitation, hourly observational records were obtained from the Brazilian National Institute of Meteorology (INMET) database (https://bdmep.inmet.gov.br, accessed on 1 July 2025) and aggregated to monthly precipitation totals for the period 1980–2024. This monthly series was used to characterize the regional precipitation regime and to support regime-scale comparisons over the MRB. To ensure spatial consistency between precipitation and reanalysis-based aerosol estimates, the MERRA-2 grid cell used in this study was centered on the INMET station location, as indicated in Figure 1.

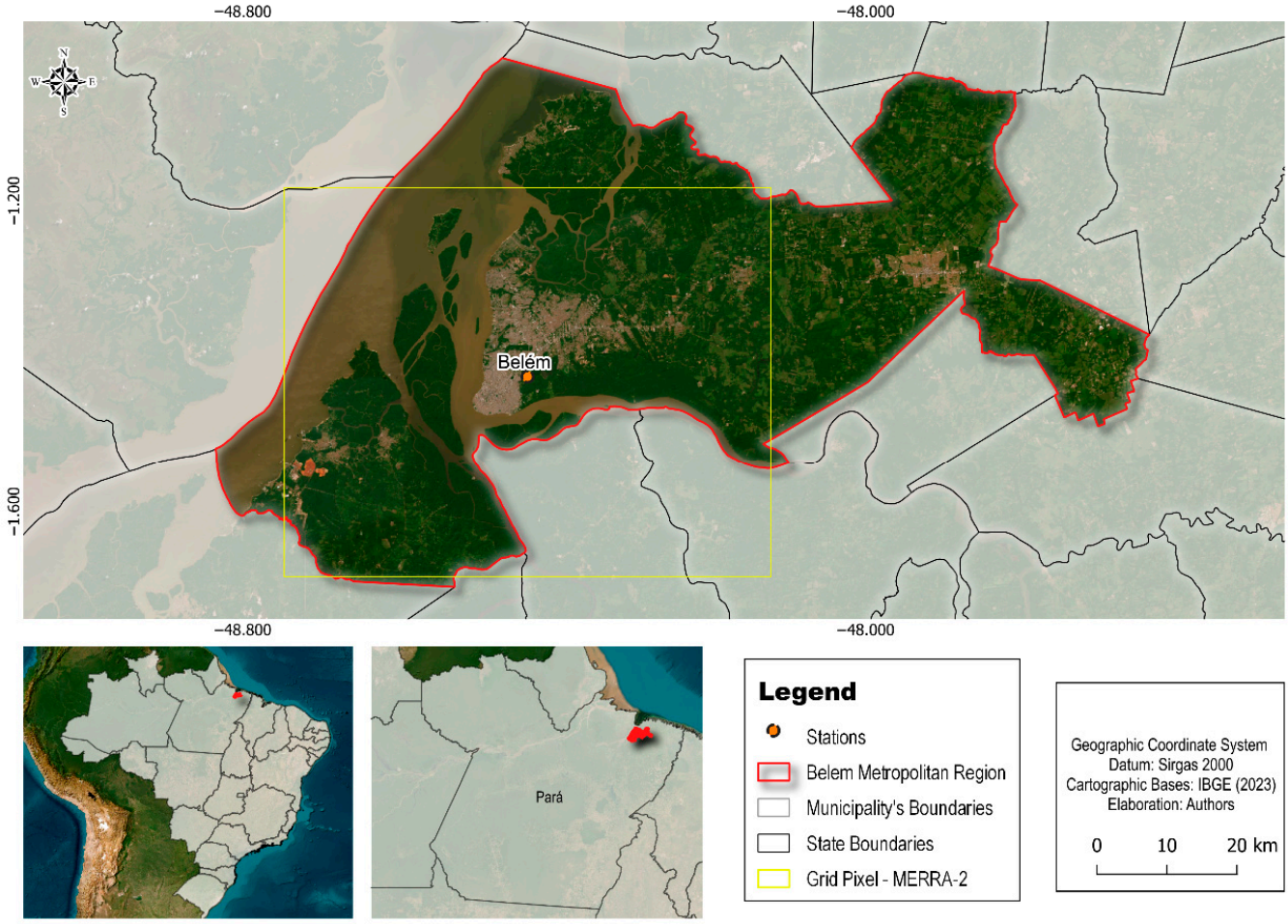

Figure 1. Geographic location of the study area. Emphasis is placed on the pixel cutout from the MERRA-2 reanalysis, from which aerosol data were extracted, and on the INMET website coordinates from which precipitation measurements were extracted.

2.2. $PM_{2.5}$ Estimates from MERRA-2 and Correction for Bias

$PM_{2.5}$ estimates from the Modern-Era Retrospective Analysis for Research and Applications, version 2 (MERRA-2), were extracted for the reanalysis grid cell centered on the INMET meteorological station coordinates, as shown in Figure 1. MERRA-2 is produced by NASA's Global Modeling and Assimilation Office (GMAO) and is available at https://gmao.gsfc.nasa.gov/reanalysis/MERRA-2 (accessed on 1 July 2025). The product has a spatial resolution of 0.5° × 0.625° [18,19]. For this study, hourly MERRA-2 data were extracted from January 1980 to December 2024 and subsequently aggregated to daily and monthly averages for analysis.

MERRA-2 uses the Goddard Earth Observing System, version 5 (GEOS-5), as the atmospheric model, interactively coupled to the Goddard Chemistry, Aerosol, Radiation and Transport (GOCART) model [29]. The GEOS-5 data assimilation system ingests multiple observation sources, including ground-based AERONET measurements and satellite retrievals from sensors such as MODIS, MISR, and AVHRR. In addition to globally validated aerosol optical properties [30], MERRA-2 provides estimates of black carbon (BC) and simulates dust (DU) and sea salt (SS) in five size ranges [31], as well as sulfate (SO_4) and organic carbon (OC) [31–33]. $PM_{2.5}$ concentrations were calculated following Equation (1) [9,12,19]:

$$PM_{2.5} = [DU_{2.5}] + 1.4[OC] + [BC] + [SS_{2.5}] + 1.375[SO_4], \quad (1)$$

where [$DU_{2.5}$], [OC], [BC], [$SS_{2.5}$], and [SO_4] represent the mass concentrations of dust, organic carbon, black carbon, sea salt, and sulfate aerosol components (diameter $\leq$ 2.5 μm), respectively. In addition to global and regional validations of MERRA-2 aerosol products, we highlight the good performance of MERRA-2 $PM_{2.5}$ estimates for local analysis in the Southern Amazon Basin [9].

To improve the reliability of the MERRA-2 $PM_{2.5}$ estimates, a bias-correction procedure based on the methodology proposed by Nassarden et al. [9] was applied, using local observational data from the Southern Amazon Basin as a reference. The correction aimed to reduce the systematic overestimation commonly reported in reanalysis products when compared to surface measurements. The bias-corrected $PM_{2.5}$ was obtained using a linear fit model given by Equation (2):

$$PM_{2.5}\text{Bias Corrected} = 0.5PM_{2.5}\text{MERRA2} + 1.6, \quad (2)$$

where $PM_{2.5}$MERRA2 represents the original estimates of MERRA-2, and the coefficients a and b were derived from the regression between the reanalysis data and the soil observations reported by Nassarden et al. [9]. The correction showed robust performance (R^2 = 0.86; correlation r = 0.92; p-value < 0.001), indicating a substantial improvement in agreement with the observed concentrations. This approach preserves the temporal variability of the original dataset while reducing magnitude-related biases, enabling more accurate interpretation of long-term trends and regime-based comparisons.

2.3. Analysis Methods

Boxplot analyses were used as an exploratory statistical tool to describe the distribution of $PM_{2.5}$ concentrations under different conditions. The boxplots summarize the median, interquartile range (IQR), and extreme values, providing a robust visualization of variability and dispersion without assuming normality of the data. The box represents the 25–75% interquartile range (IQR), and potential outliers defined as values exceeding 1.5 × IQR. Figure S1 (Supplementary Material) illustrates the graphical structure of the boxplot used in this study, including the representation of quartiles, whiskers, and outliers. This approach is particularly useful for identifying differences between precipitation regimes and seasonal patterns in $PM_{2.5}$ distributions. A supplementary analysis was conducted in which $PM_{2.5}$ concentrations, bias-corrected, were used to calculate the Air Quality Index (AQI) based on guidelines from the United States Environmental Protection Agency (EPA), adapted to the Brazilian context [34].

2.3.1. Trend Analysis Using the Mann–Kendall (MK) Test

Temporal trends in precipitation and $PM_{2.5}$ concentrations were assessed using the non-parametric Mann–Kendall (MK) test, which is widely applied in hydroclimatic and environmental studies due to its robustness to non-normal data distributions and reduced sensitivity to outliers. The MK test evaluates the presence of a monotonic trend (increasing or decreasing) in a time series without requiring assumptions of linearity or data normality. The test statistic (S) is computed based on the relative ordering of all possible pairs of observations in the time series. From S, the standardized test statistic (Z) is derived to evaluate statistical significance. Positive Z values indicate increasing trends, while negative values indicate decreasing trends. The strength and direction of the trend are further quantified using Kendall's tau (τ), a rank-based correlation coefficient ranging from −1 to +1. The statistical significance of the trends was assessed at the 5% (p < 0.05) and 1% (p < 0.01) levels.

To estimate the magnitude of the detected trends, Sen's slope estimator was applied, providing a robust measure of the rate of change over time (e.g., μg m^{-3} $year^{-1}$ for $PM_{2.5}$

and mm year^{-1} for precipitation). All analyses were performed on monthly aggregated time series, considering both the full period and subsets defined by precipitation regimes (e.g., dry, normal, and wet classes).

In addition, linear regression (LR) was applied to evaluate the association between Standardized Precipitation Index (SPI) values and $PM_{2.5}$ concentrations at the monthly (regime) scale. Regression results were evaluated using their respective *p*-values; relationships with *p*-value < 0.05 were considered significant and those with *p*-value < 0.01 were considered highly significant. The distributional properties used to support inference were assessed using the Kolmogorov–Smirnov, Anderson–Darling, and Epps–Singleton methods. All analyses and statistical tests were performed using the Statsmodels module (version 0.14.x) in Python. These regressions are interpreted as statistical associations in monthly aggregated series and do not, by themselves, imply event-scale causal effects. The graphical analyses were performed using Matlab 2025b.

2.3.2. Standardized Precipitation Index (SPI)

The Standardized Precipitation Index (SPI) is an index used to assess how precipitation varies relative to the climatology of the period considered. Positive SPI values indicate above-average precipitation, whereas negative values indicate below-average precipitation. In this study, SPI was calculated at a monthly resolution (i.e., a 1-month time scale) using Equation (3), allowing a regime-scale classification of precipitation conditions:

$$\mathrm{SPI} = \frac{\mathrm{P_i} - \overline{\mathrm{P_o}}}{\sigma_\mathrm{i}}, \tag{3}$$

where i is the time scale; P_i is the observed precipitation; $\overline{P_o}$ and σ_i are the mean and standard deviation of the series, respectively. The SPI was used to identify dry and wet conditions across the study period. Table 1 summarizes the SPI categories according to McKee et al. [35].

Table 1. Classification of dry and wet periods of the SPI (McKee et al. [35]).

SPI Values	Category
<−2.0	ExD = Extreme Drought
−1.99 to −1.50	SeD = Severe Drought
−1.49 to −1.0	MoD = Moderate Drought
−0.99 to −0.49	MiD = Mild Drought
−0.49 to 0.49	NN = Near Normal
0.49 to 0.99	LiR = Light Rainfall
0.99 to 1.49	MoR = Moderate Rainfall
1.49 to 1.99	SeR = Severe Rainfall
>2.0	ExR = Extreme Rainfall

The SPI was then used to quantify the number of months in each category and to evaluate variations in $PM_{2.5}$ concentration under distinct precipitation regimes. For subsequent analyses, SPI categories were consolidated into three groups: wet (ExR, SeR, MoR, and LiR), normal (NN), and dry (ExD, SeD, MoD, and MiD). This grouping enabled comparisons of $PM_{2.5}$ mean concentrations among the three precipitation regimes using Student's *t*-test.

2.3.3. *t*-Test for Comparison of Means

Pairwise comparisons of $PM_{2.5}$ mean concentrations among precipitation regimes (dry, normal, and wet) were performed using Student's *t*-test. Differences between groups were also evaluated using the Mann–Whitney, Mood median, Kolmogorov–Smirnov,

Anderson–Darling, and Epps–Singleton tests. Statistical significance was assessed at the 0.05 (p-value < 0.05) and 0.01 (p-value < 0.01) levels. For p-values below the chosen thresholds, the null hypothesis (H_0) of equality between group means was rejected, indicating statistically significant or highly significant differences.

The t-tests were applied in pairs for $PM_{2.5}$ conditions: dry vs. normal, dry vs. wet, and normal vs. wet. Although the t-test is typically recommended for data that follow an approximately normal distribution, here inference on mean differences was supported by the Central Limit Theorem, which states that the sampling distribution of the mean approaches normality for sufficiently large samples (n > 30), even when the underlying data are not normally distributed. Figure 2 summarizes the methodological workflow adopted in this study.

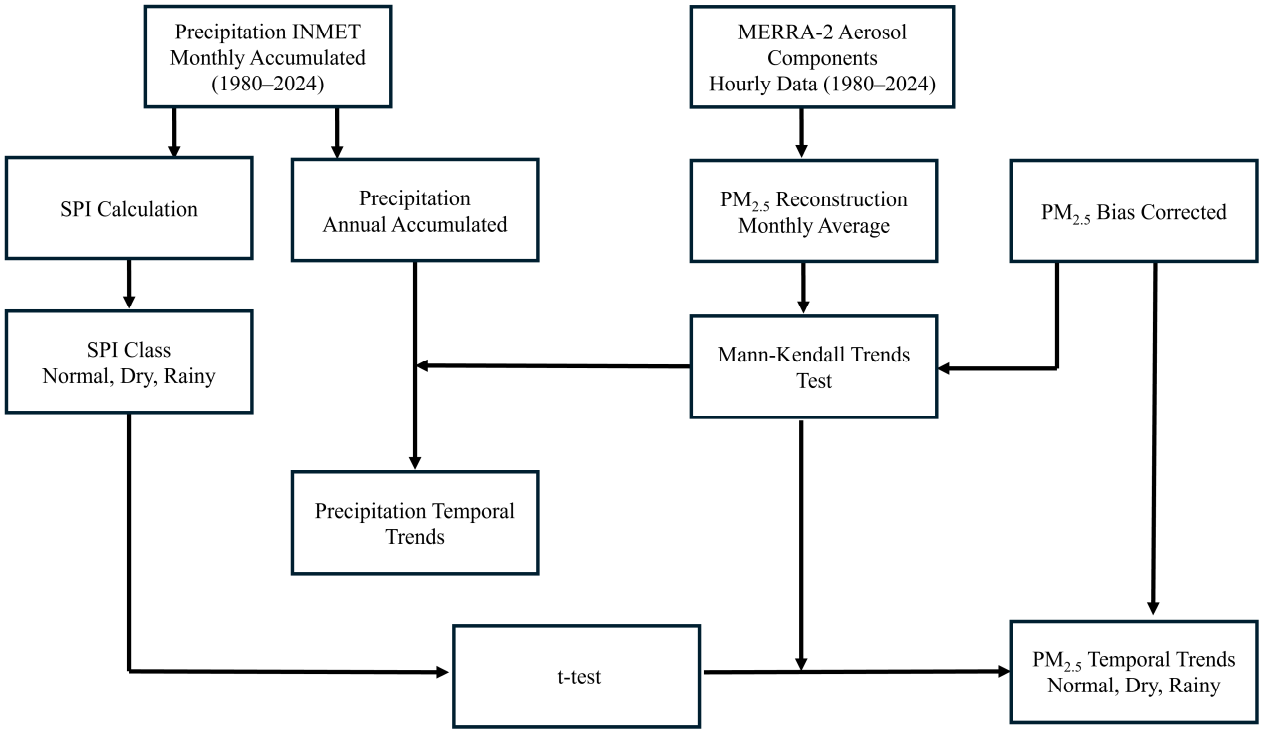

Figure 2. Schematic approach for the analysis of precipitation, and $PM_{2.5}$ trends, and for deriving $PM_{2.5}$ time series for normal, wet, and dry precipitation regimes.

3. Results

3.1. Trend of Increasing Annual Precipitation in the Metropolitan Region of Belém

Figure 3a compares monthly precipitation climatological normals for Belém (1961–1990, 1981–2010, and 1991–2020) with the study-period series (1980–2024) based on measurements from the conventional Belém weather station. Overall, the monthly patterns are consistent across periods, indicating a stable and well-defined annual precipitation cycle in the region. This cycle includes transition months [26] and supports the division between a wet season (December to May) and a dry or less wet season (June to November) [28].

For Belém, the seasonal precipitation structure is unimodal and strongly seasonal, with the wet-season months concentrated in the first part of the year and markedly lower precipitation during the second half of the year [28]. When comparing the study period with the climatological normals, the largest contrasts are concentrated around the peak wet-season month: relative to the oldest normal (1961–1990), the study-period peak appears lower on the order of ~10–15%, whereas differences relative to the more recent normals (1981–2010 and 1991–2020) are comparatively small (generally within a few percent), sug-

gesting broadly similar peak-season behavior in recent decades. Minor departures from the shared seasonal pattern are also apparent in late-wet/early-transition months (e.g., May) and at the start of the wet season (e.g., December), consistent with modest shifts in the timing and/or intensity of monthly rainfall within the same unimodal regime.

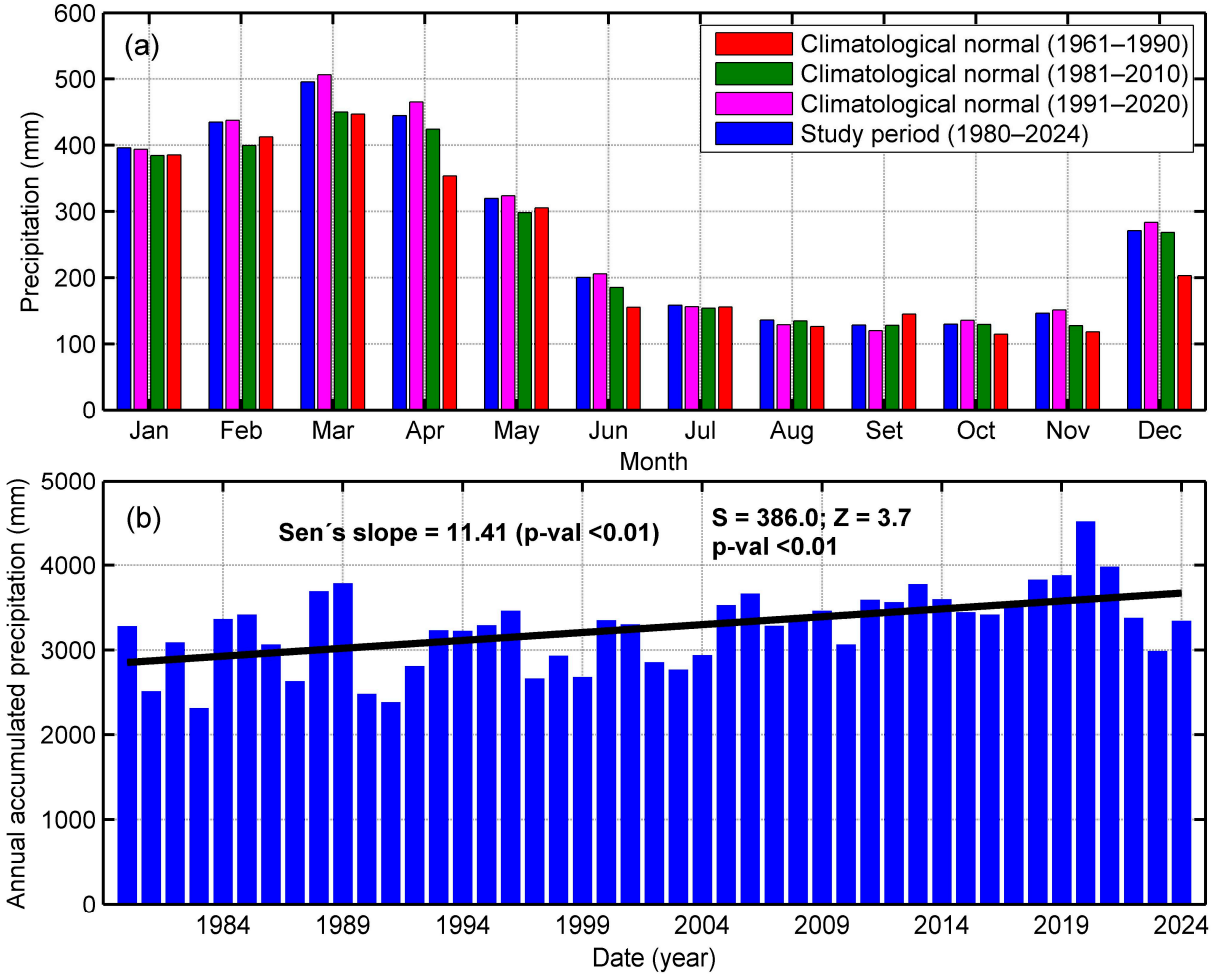

Figure 3. (**a**) Comparison of monthly accumulated precipitation for the study period (1980–2024) with the climatological normals for 1961–1990, 1981–2010, and 1991–2020 in Belém (PA). (**b**) Time series of annual accumulated precipitation (1980–2024) in the Metropolitan Region of Belém (MRB), including the linear trend.

Figure 3b shows the annual accumulated precipitation series for the study period and indicates substantial interannual variability, with wetter years reaching roughly ~70–90% higher annual totals than drier years. Despite this variability, both the Mann–Kendall (MK) test and the complementary linear regression analysis indicate a statistically significant increasing trend in annual precipitation over 1980–2024. This result is consistent with previous evidence for increasing precipitation in Belém and suggests that long-term changes in rainfall have occurred alongside the maintained strong seasonality of the regional precipitation regime [28,36].

3.2. $PM_{2.5}$ Concentration

The comparison between the original and bias-corrected $PM_{2.5}$ datasets (Figure 4) is consistent with the validation framework adopted in this study. As described in the methodology, bias correction was designed to reduce systematic deviations while preserving the temporal structure of the MERRA-2 product. In the time series (Figure 4a), the corrected

data shows a clear reduction in magnitude compared to the original dataset, with fewer extreme values and a narrower variability range. However, both series maintain similar temporal patterns, including interannual variability and periods of high concentrations. This indicates that the correction effectively adjusts the amplitude of $PM_{2.5}$ concentrations without distorting the underlying temporal signal, in accordance with the expected behavior of the applied correction method.

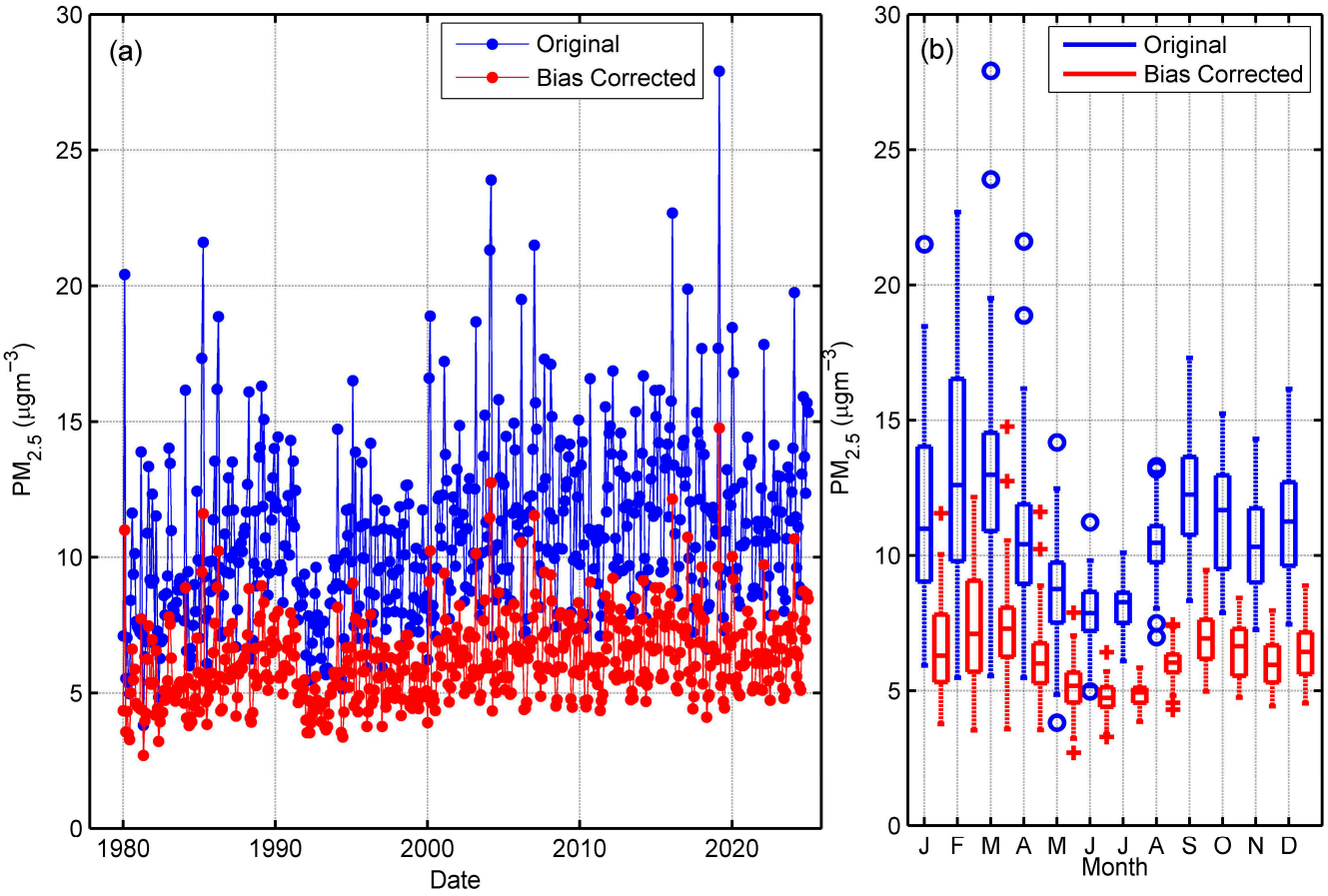

Figure 4. (**a**) Time series for the monthly values of $PM_{2.5}$, original from MERRA-2 and corrected for bias. (**b**) Boxplot with the monthly variations in $PM_{2.5}$, original from MERRA-2 and corrected for bias.

Seasonal analysis (Figure 4b) further confirms the validity of bias correction. While the original dataset shows higher medians, larger interquartile ranges, and more frequent outliers in most months, the corrected dataset shows a tighter distribution and reduced dispersion. Despite these differences, the seasonal cycle remains consistent between the two datasets, demonstrating that the correction preserves relative monthly variability while improving the quantitative representation of $PM_{2.5}$ concentrations. This behavior is consistent with the validation results presented in the methodological section, confirming that bias correction increases the reliability of the dataset for subsequent statistical analyses without altering its fundamental seasonal and temporal characteristics.

Figure 5 shows the monthly statistics and time series for the annual averages of $PM_{2.5}$ concentration (μgm^{-3}); values are corrected for bias [9]. Consistently, the bimodal seasonal behavior and the positive long-term trend are maintained after correction (Figure 5). In relative terms, the bias correction dampens the long-term linear increase in annual $PM_{2.5}$ by approximately one-half and reduces the baseline level by about two-fifths, while preserving the same overall trajectory (Figures 4b and 5).

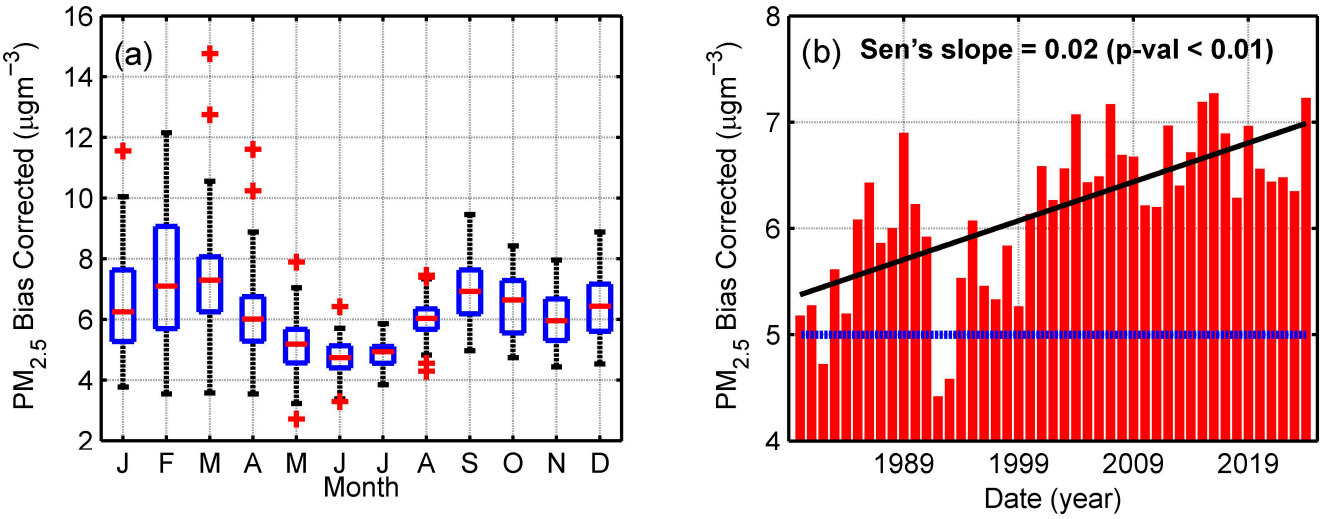

Figure 5. (**a**) Monthly boxplots of bias-corrected $PM_{2.5}$ concentrations from MERRA-2 (1980–2024). (**b**) Time series of annual mean bias-corrected $PM_{2.5}$ (1980–2024), including the WHO annual guideline reference line.

For $PM_{2.5}$, it is possible to observe two waves of higher concentrations (Figure 5a). These results were, at first, unexpected, since the first wave, with medians around 13 μgm^{-3}, was obtained for March (Figure 5a), a period corresponding to the highest rainfall intensity in the region. It is important to emphasize that, since these results are derived from monthly aggregates, this pattern indicates that months with higher precipitation may still coincide with high $PM_{2.5}$ distributions in the wet season; however, we cannot say that individual precipitation events are unable to remove particles.

Monthly boxplots further reveal that variability is not uniform throughout the year, with certain months exhibiting larger interquartile ranges and more frequent extreme values, reflecting changes in atmospheric processes and aerosol composition.

Although the focus of this study is the concentration of fine particulate matter, Figure 6 shows the monthly variations in the aerosol constituents obtained from MERRA-2, because examining specific fractions helps interpret the overall variation in $PM_{2.5}$. The results show distinct monthly behavior across aerosol categories and clear differences in relative magnitude. In particular, $DU_{2.5}$ and $SS_{2.5}$ exhibit concentrations that are roughly an order of magnitude higher than BC and SO_4, whereas OC shows intermediate levels and variability (Figure 6a–e). The constituent boxplots also show month-dependent changes in central tendency and spread, as well as occasional outliers, indicating that the $PM_{2.5}$ seasonal cycle reflects changing mixtures of aerosol components across the year.

For the second half of the year, higher $PM_{2.5}$ concentrations, peaking in September (Figure 5a), occur concurrently with months when $SS_{2.5}$ remains elevated and when BC, OC, and SO_4 show increased distributions (Figure 6b–e). This co-occurrence is consistent with a period in which marine aerosol contributions and carbonaceous/sulfate components may jointly contribute to monthly $PM_{2.5}$ variability. Although BC concentrations are generally low, between September and December the upper tail of the distribution increases markedly (Figure 6b), which may have implications for radiative effects and near-surface temperature [37].

The annual time series of $PM_{2.5}$ shows a positive and highly significant trend, indicating that the increase in annual precipitation during the study period does not coincide with a long-term decreasing trend in surface $PM_{2.5}$. Figure 5b also shows that, even after bias correction, the annual averages remain above the national recommendations of CONAMA [34] and WHO [38] of 5 μgm^{-3}; over the 45 years analyzed, only three years

showed concentrations below this recommendation. The time series of the Air Quality Index (AQI) (Figure S2, Supplementary Material) also shows positive and highly significant trends. Although a positive trend was found for the AQI, its values remained within the "Good" classification of CONAMA [34] (Figure S2).

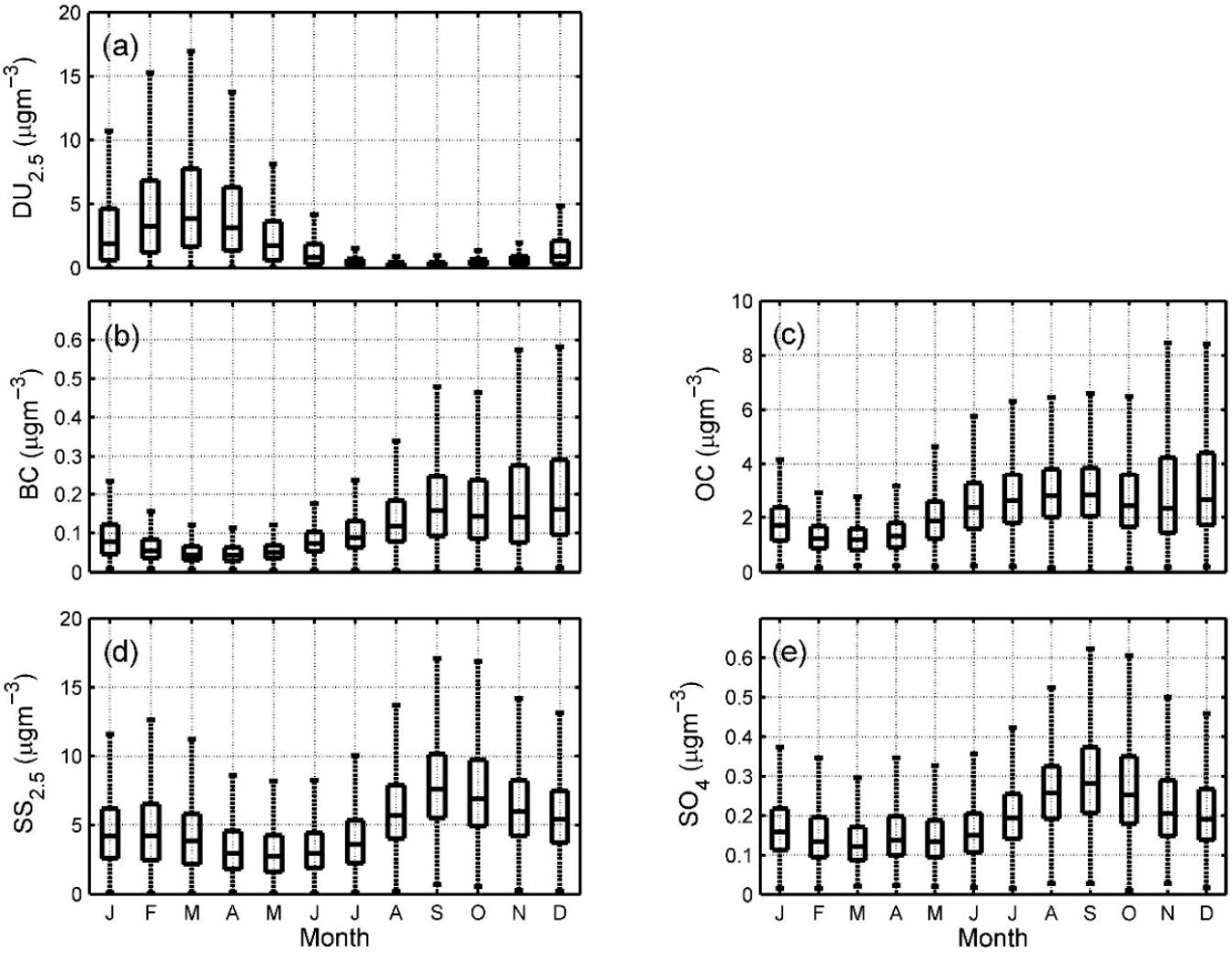

Figure 6. Monthly boxplots of MERRA-2 aerosol constituent concentrations (1980–2024): (**a**) fine dust ($DU_{2.5}$), (**b**) black carbon (BC), (**c**) organic carbon (OC), (**d**) fine sea salt ($SS_{2.5}$), and (**e**) sulfate (SO_4).

3.3. $PM_{2.5}$ Concentration for Different SPI Classes

Figure 7a shows the monthly time series of the SPI, which exhibits pronounced variability over 1980–2024, alternating between negative (drier-than-normal) and positive (wetter-than-normal) conditions. This SPI series was used to classify months into precipitation categories following the SPI thresholds described in Section 2.3.3. The frequency of occurrence for each SPI class is summarized in Figure 7b and indicates a clear predominance of near-normal (NN) and mild drought (MiD) conditions, which together account for more than half of the months in 1980–2024. Notably, no month was classified as extreme drought (ExD) during the study period (Figure 7b). In contrast, the wetter tail of the distribution is less frequent, with the severe and extreme rainfall classes (SeR and ExR) representing a relatively small fraction of all months (approximately one-tenth, as quantified in the class counts), consistent with rainfall extremes being episodic rather than the prevailing regime.

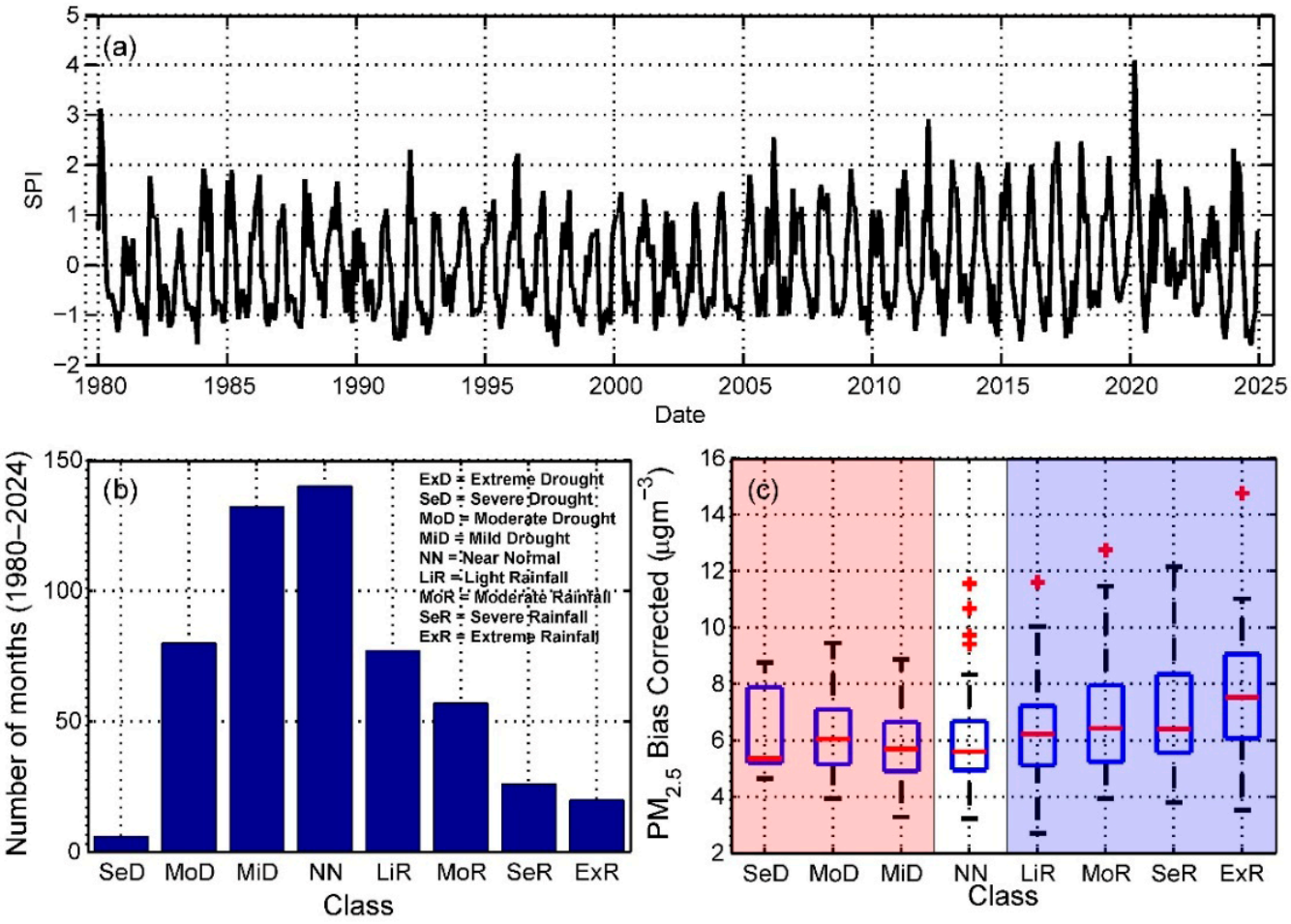

Figure 7. (**a**) Monthly time series of the Standardized Precipitation Index (SPI) for the study period. (**b**) Number of months classified into each SPI category over 1980–2024. (**c**) Boxplots of bias-corrected $PM_{2.5}$ concentrations by SPI class (SeD, MoD, MiD, NN, LiR, MoR, SeR, ExR).

Figure 7c presents boxplot statistics of bias-corrected $PM_{2.5}$ by SPI class and shows substantial overlap among class distributions, together with class-dependent differences in dispersion and upper-tail behavior. In general, the wettest classes (SeR/ExR) display higher central values and a more pronounced upper tail than most dry and near-normal classes, including several high-end outliers. Conversely, the more frequent classes (NN and MiD) show comparatively tight central distributions but still exhibit occasional elevated outliers, indicating that high $PM_{2.5}$ episodes are not restricted to a single SPI category. Consistent with Figure 5, the class-specific patterns in Figure 7c reinforce that higher $PM_{2.5}$ months can co-occur with wetter SPI conditions at the monthly (regime) scale.

For subsequent analysis, SPI classes were consolidated into three broader groups: dry (SeD + MoD + MiD), normal (NN), and wet (LiR + MoR + SeR + ExR). The resulting distributions are summarized in Figure 8a and complemented in Table 2. Figure 8a shows that the wet group has a slightly higher central tendency and a more elevated upper tail than the other groups, whereas the dry and normal groups are highly similar in their central ranges. These visual patterns are consistent with Table 2, where all statistical tests converge on a highly significant difference between the wet class and the other classes, while no significant difference is detected between dry and normal conditions.

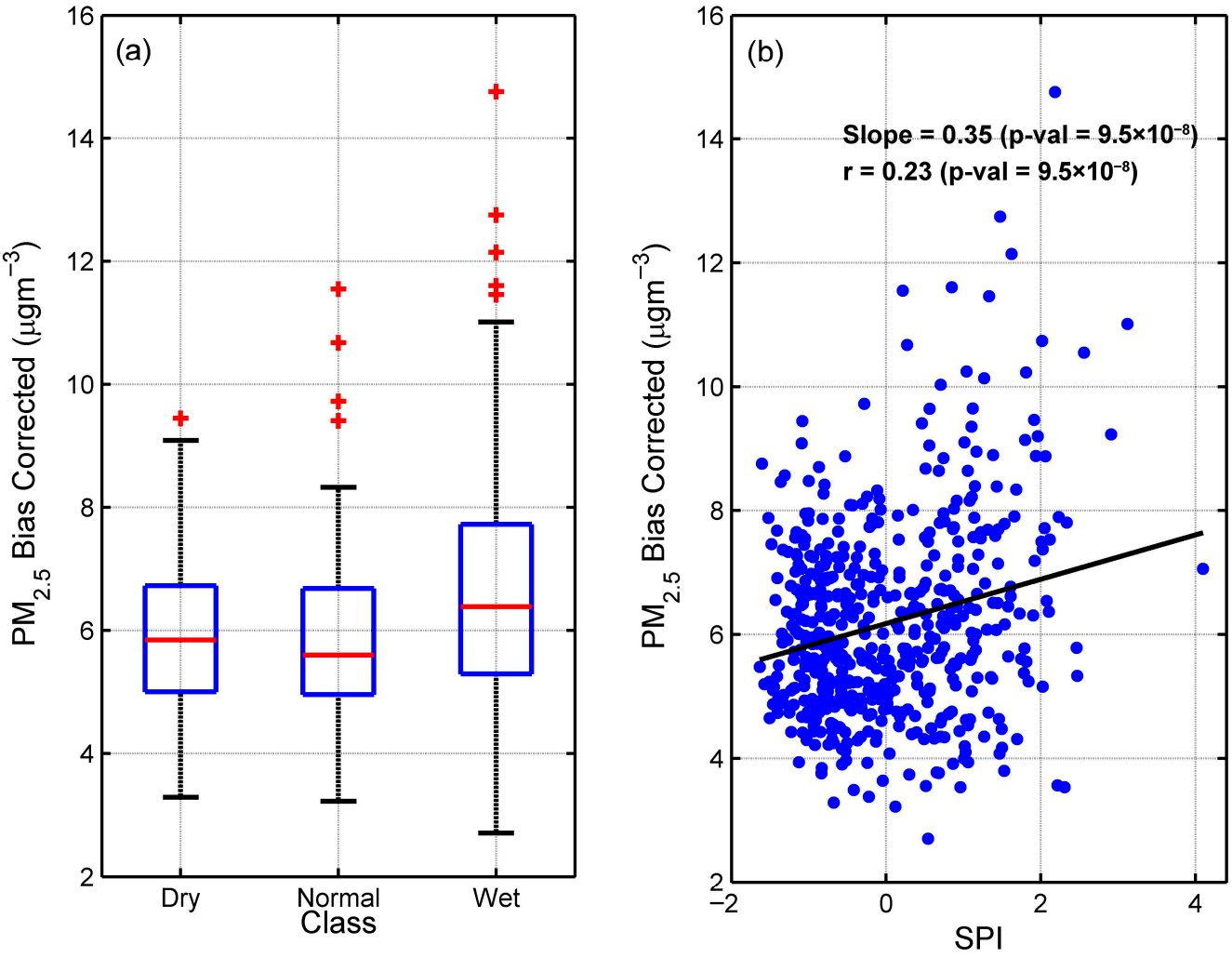

Figure 8. (**a**) Boxplots comparing bias-corrected $PM_{2.5}$ concentrations across aggregated precipitation regimes (dry, normal, and wet) derived from SPI classes. (**b**) Scatterplot showing the linear relationship between SPI and bias-corrected $PM_{2.5}$, including the fitted regression line and associated statistics.

Table 2. Descriptive statistics of bias-corrected $PM_{2.5}$ concentrations (μgm^{-3}) under aggregated precipitation regimes (dry, normal, and wet) and pairwise comparisons of group means. Mean differences were tested using Student's *t*-test, and distributional differences were evaluated using the Mann–Whitney, Mood median, Kolmogorov–Smirnov, Anderson–Darling, and Epps–Singleton tests. Superscripts indicate statistical significance: [a], *p*-value > 0.05; [b], *p*-value < 0.01.

	Descriptive			**Differences**		
	Dry	**Normal**	**Wet**	**Dry-Normal**	**Dry-Wet**	**Normal-Wet**
N	218	140	180	-	-	-
Median	5.84	5.60	6.38	-	-	-
Mean	5.95	5.92	6.66	0.03 [a]	−0.71 [b]	−0.73 [b]

Figure 8b further indicates a positive but weak linear association between SPI and bias-corrected $PM_{2.5}$, characterized by substantial scatter around the regression line. The correlation coefficient and slope reported in Figure 8b are statistically significant, supporting an overall tendency for $PM_{2.5}$ to increase with increasing SPI while emphasizing that SPI alone explains only a limited fraction of $PM_{2.5}$ variability at the monthly scale.

The correlation analysis between precipitation and $PM_{2.5}$ revealed a regime-dependent behavior, highlighting the importance of stratifying the dataset according to precipitation

classes (Figure 9). For the entire period (Figure 9a), a weak but statistically significant positive correlation is observed (r = 0.23, $p < 0.01$), indicating that higher precipitation levels are, on average, associated with slightly higher $PM_{2.5}$ concentrations on a monthly scale. A similar pattern is found for the wet class (Figure 9c), where the correlation remains positive and significant (r = 0.24, $p < 0.01$), suggesting that, under wetter conditions, precipitation does not necessarily lead to a reduction in particulate matter concentrations.

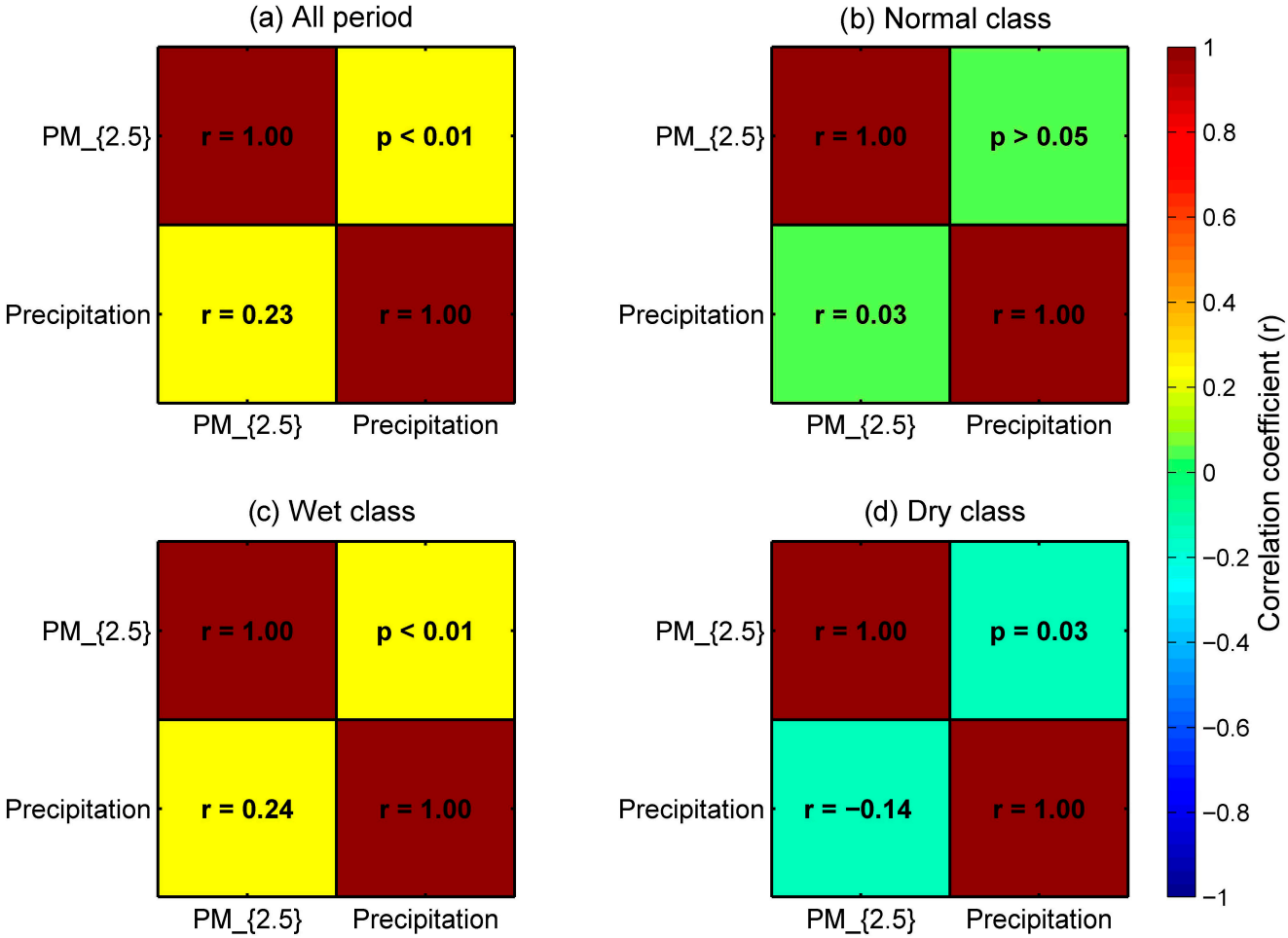

Figure 9. Correlation matrices between $PM_{2.5}$ concentration and precipitation for different precipitation regimes in the Metropolitan Region of Belém. Panels represent (**a**) the entire period, (**b**) normal conditions, (**c**) wet conditions, and (**d**) dry conditions. Each matrix shows Pearson correlation coefficients (r), with corresponding *p*-values indicated for off-diagonal elements. Color shading represents the strength and direction of the correlation, ranging from −1 (negative) to +1 (positive). Diagonal elements represent autocorrelation (r = 1).

In contrast, the normal class (Figure 9b) exhibits a relationship close to zero and not significant (r = 0.03, $p > 0.05$), indicating a weak coupling between precipitation and $PM_{2.5}$ under intermediate conditions. A distinct behavior emerges in the dry class (Figure 9d), where a weak negative correlation is identified (r = −0.14, $p = 0.03$), suggesting that precipitation events during drier periods are more effective in reducing $PM_{2.5}$ concentrations. This contrast between wet and dry classes reinforces that the precipitation–$PM_{2.5}$ relationship is not linear and depends on prevailing atmospheric conditions. Specifically, while precipitation under dry conditions appears to increase particulate removal, wetter regimes may be associated with processes that maintain or even increase $PM_{2.5}$ levels on a monthly scale. Overall, these results demonstrate that the interaction between precipitation and particu-

late matter is strongly modulated by precipitation, emphasizing the need for precipitation class-based analyses when interpreting relationships between aerosols and meteorology.

3.4. Trends in $PM_{2.5}$ Concentration

The application of the Mann–Kendall (MK) test to the $PM_{2.5}$ time series is shown in Figure 10. For the normal (Figure 10a) and wet (Figure 10c) classes, positive and statistically significant trends were identified for $PM_{2.5}$ concentration. In contrast, for the dry class (Figure 10b), the fitted trend is weak and the MK test indicates no statistically significant trend. These class-stratified results are consistent with the overall increasing tendency in $PM_{2.5}$ previously observed (Figure 5b) and indicate that the long-term increase is primarily reflected under the normal and wet regimes, whereas the dry regime does not show a detectable trend over the study period.

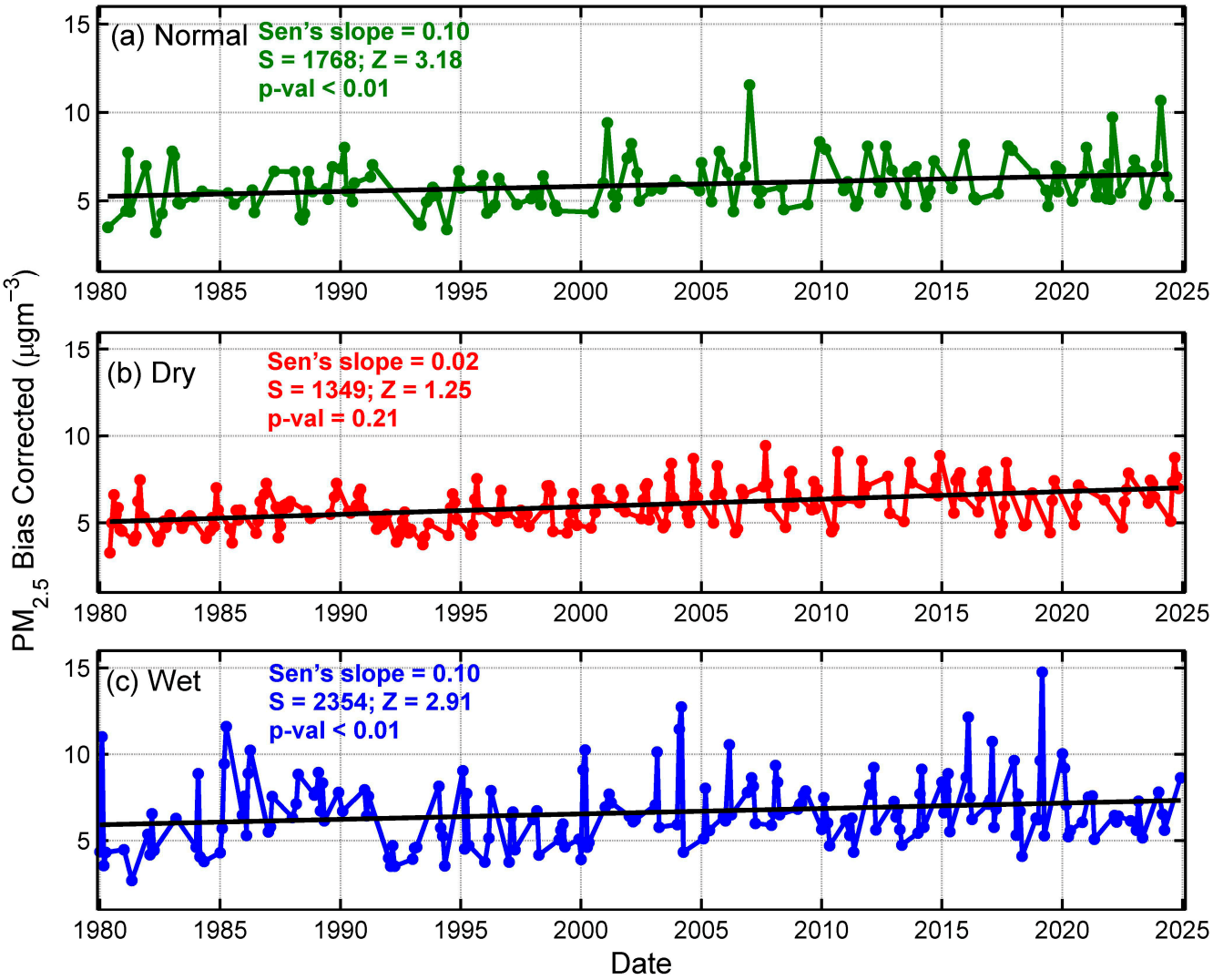

Figure 10. Time series of bias-corrected $PM_{2.5}$ concentrations by aggregated SPI-derived precipitation regime: (**a**) normal, (**b**) dry, and (**c**) wet. Each panel shows the class-specific temporal series and the fitted linear trend line, together with the corresponding Mann–Kendall trend statistics (S, Z, and *p*-value) and regression slope with its *p*-value.

Although this pattern may appear counterintuitive, recent evidence from different regions indicates that precipitation–particulate matter associations can be context-dependent, with mixed or even positive relationships reported in some settings [20,22,39–41]. For example, studies in Africa and China have highlighted that, depending on regional atmospheric

conditions, transport, and secondary processes, wetter regimes may not systematically coincide with lower monthly $PM_{2.5}$ levels [20,40,41].

4. Discussion

Evidence from other regions indicates that the precipitation–$PM_{2.5}$ relationship is not uniformly negative. In Africa, Ouma et al. [20] reported an average reduction in particulate matter in wet environments, yet also found weak and even positive precipitation–$PM_{2.5}$ correlations in regional analyses, particularly over northern and eastern Africa, consistent with the influence of convective regimes and atmospheric transport during wet periods [20]. Omokpariola [41] further noted that intervals between precipitation events can facilitate PM accumulation and affect seasonal averages. In China, soil moisture and a humid atmosphere have been identified as important modulators of secondary $PM_{2.5}$ formation; wet conditions can reduce mineral dust while simultaneously favoring secondary aerosol production [40].

For eastern Amazonia, previous studies have reported positive precipitation trends [28,36,42,43]. Souza et al. [28] highlighted that, in addition to increasing accumulated precipitation in Belém, extremely high precipitation events have become more frequent, and their average magnitude has increased by around 23 mm during the wet season. They associated these changes with land-use transitions, arguing that urbanized areas favor heating and local convection, which can intensify rainfall. Costa et al. [42] emphasized the influence of warming South Atlantic waters on precipitation regimes in eastern Amazonia, pointing to the role of the tropical Atlantic in modulating the position of the Intertropical Convergence Zone (ITCZ) and amplifying conditions favorable for deep convection, in the context of regional environmental change and global climate warming. Climate teleconnections also strongly modulate regional convective systems [43]. Accordingly, the observed increase in precipitation may reflect the combined effects of Atlantic Multidecadal Oscillation (AMO), El Niño–Southern Oscillation (ENSO), and Pacific Decadal Oscillation (PDO), together with land-use change and local/regional atmospheric warming. In particular, the positive phase of the AMO has been described as an important factor intensifying the ITCZ and deep convection over eastern Amazonia, generating more intense, frequent, and prolonged rainfall [43].

These climate and circulation patterns may also help contextualize the first wave of increased $PM_{2.5}$ concentrations in the first half of the year. Rodrigues et al. [44] showed that, in the first months of the year, air-mass trajectories reaching southern Pará are directly influenced by transport pathways from northern Africa, implying that elevated $PM_{2.5}$ during this period may largely reflect contributions commonly considered of natural origin. Consistently, Faria et al. [45] argued that much of the particulate matter variability in eastern Amazonia during the wet season is strongly modulated by long-distance aerosol transport from Africa, with the ITCZ latitudinal position defining an "atmospheric corridor" that can favor or inhibit dust plume penetration into the tropical Atlantic. When the ITCZ moves southward (DJF–MAM), aerosols preferentially cross the ocean between 0° and 10° N, directly connecting the eastern tropical Atlantic to northern South America [45]. Gutleben et al. [46] further described that during Harmattan episodes (late November to mid-March) dust plumes can follow near-horizontal trajectories over the Atlantic, facilitating arrival in South America when the ITCZ is farther south; in such episodes, dust, often mixed with wildfire aerosols from Central Africa, may alter aerosol optical and hygroscopic properties and potentially increase $PM_{2.5}$ levels in eastern Amazonia [46].

At the same time, precipitation events are not solely associated with atmospheric cleansing. Studies by Li et al. [24], Almeida et al. [39], and Zhou et al. [23] showed that precipitation can coincide with increased particulate matter concentrations under

certain atmospheric conditions and aerosol physicochemical properties. In this framework, increases in *PM* mass concentration may occur through hygroscopic growth under higher relative humidity [39,47] and through accelerated formation of secondary aerosols during and after precipitation events [23]. Zhou et al. [23] reported that, at intermediate-to-high relative humidity, hygroscopic growth can dominate over wet removal, increasing $PM_{2.5}$ mass; higher humidity can also favor aqueous and heterogeneous reactions producing sulfates and nitrates, and, combined with low wind speed and light rain, can provide conditions conducive to fine-particle growth [23].

Positive trends in $PM_{2.5}$ have also been reported elsewhere, including across multiple regions of Brazil, commonly discussed in relation to biomass burning in rural areas, land-cover change, and intensification of urban activities [5,6,9,48]. In Belém, a positive trend in $PM_{2.5}$ may also relate to urbanization, with associated vegetation loss and wind suppression [28]. These results reflect the combined influence of transport processes and secondary aerosol formation mechanisms discussed above [24,39,49,50]. Importantly, the regime-based separation of data does not support the statement that $PM_{2.5}$ concentrations are necessarily higher during the climatological "wet season" defined by monthly precipitation averages. Rather, the analysis evaluates how precipitation-event regimes (SPI-derived classes) relate to concentration levels and trends. Therefore, the finding that $PM_{2.5}$ mass concentrations are statistically higher in the "wet class" is not equivalent to stating that $PM_{2.5}$ is higher throughout the climatological wet season, because month-based seasonal averaging over years may lead to a different result.

In this context, we observe positive $PM_{2.5}$ trends in the wet class in the urban area of Belém (Figure 10c). This interpretation is consistent with the correlation analysis, which shows a weak, but statistically significant, positive relationship between precipitation and $PM_{2.5}$ in the wet class ($r = 0.24$, $p < 0.01$). Taken together, these results indicate that, on a monthly scale, higher levels of precipitation can coexist with high $PM_{2.5}$ concentrations under wet conditions. Within this context, the observed positive association between precipitation and $PM_{2.5}$ under humid conditions aligns with findings reported in regions of Africa, China, and other tropical urban environments [20,40,41], reinforcing that precipitation alone is not a sufficient predictor of reduced particulate matter concentrations.

Trend analysis based on the Mann–Kendall test and the Sen slope estimator (Table 3) reveals consistent, but class-dependent, increases in both precipitation and $PM_{2.5}$ over the study period. For precipitation, a strong, statistically significant increasing trend was observed for the total period ($\tau = 0.82$, $Z = 28.38$, p-value < 0.01), with a Sen slope of 11.41 mm year^{-1}, indicating a substantial intensification of precipitation over time. This positive trend is also evident in the wet ($\tau = 0.70$, p-value < 0.01) and dry ($\tau = 0.50$, p-value < 0.01) classes, with slopes of 16.38 and 5.53 mm year^{-1}, respectively, highlighting that both extremes for the precipitation classes are becoming more pronounced. In contrast, the normal class does not show a statistically significant trend (p-value = 0.92), suggesting relative stability under intermediate precipitation conditions.

For $PM_{2.5}$, the results indicate a weaker, but still significant, increasing trend for the total period ($\tau = 0.12$, $Z = 4.28$, p-value < 0.01), with a slope of 0.021 μgm^{-3} year^{-1}. This positive trend is also observed in the normal ($\tau = 0.182$, p-value < 0.01) and wet ($\tau = 0.14$, p-value < 0.01) classes, with slopes of 0.10 μgm^{-3} year^{-1}, indicating that $PM_{2.5}$ concentrations are increasing even under wetter conditions. However, no statistically significant trend was detected in the dry class (p-value = 0.21), suggesting that the variability of $PM_{2.5}$ in drier regimes may be more influenced by episodic processes than by long-term changes. Taken together, these results reinforce the idea that increased precipitation does not necessarily lead to a reduction in $PM_{2.5}$ on a monthly scale. Instead, both variables exhibit concomitant positive trends, particularly under humid conditions, strengthening

the interpretation that the interactions between aerosols and precipitation in the region are complex and modulated by processes specific to each precipitation class, rather than simple mechanisms of wet removal.

Table 3. Summary of results of the Mann–Kendall trend test applied to monthly time series of precipitation and $PM_{2.5}$, stratified by precipitation classes (total period, normal, wet, and dry). The direction and magnitude of the trend were assessed using Kendall's Tau (τ) and Sen's slope (expressed in units per year), respectively. Statistical significance was assessed at the 5% level ($p < 0.05$), with significant trends marked by an asterisk (*).

Variable	Class	N	Tau	Z	*p*-Value	Sen's Slope/Year	Trend
Precipitation	All Periods	538	0.82	28.38	0.00	11.41	Trend+ *
	Normal	140	0.00	0.09	0.92	0.12	Trend+
	Wet	180	0.70	14.08	0.00	16.38	Trend+ *
	Dry	218	0.50	10.99	0.00	5.53	Trend+ *
$PM_{2.5}$	All Periods	538	0.12	4.28	0.00	0.02	Trend+ *
	Normal	140	0.18	3.18	0.00	0.10	Trend+ *
	Wet	180	0.14	2.91	0.00	0.10	Trend+ *
	Dry	218	0.05	1.21	0.21	0.02	Trend+

5. Conclusions

Our analysis indicates that the Metropolitan Region of Belém (MRB) exhibits concurrent long-term increases in precipitation and $PM_{2.5}$ concentration over the last four decades, with higher $PM_{2.5}$ levels consistently associated with wetter precipitation regimes. These findings challenge the conventional assumption that increased rainfall necessarily leads to improved air quality in humid tropical environments.

The results indicate that, at the monthly (regime) scale, precipitation can coexist with or even favor elevated $PM_{2.5}$ concentrations, likely due to the combined effects of hygroscopic particle growth, secondary aerosol formation, and long-range transport processes. A key limitation of this study is the reliance on reanalysis-based $PM_{2.5}$ data, which, despite bias correction, may not fully capture local-scale variability. In addition, the SPI-based classification does not resolve precipitation intensity, duration, or frequency, which may influence aerosol–precipitation interactions.

Future research should integrate in situ aerosol measurements, chemical composition analyses, and higher-resolution meteorological data to better constrain the mechanisms driving $PM_{2.5}$ variability in tropical urban environments. Overall, this study provides new evidence that wet conditions in the Eastern Amazon can be associated with increased particulate matter concentrations, emphasizing the need to incorporate precipitation regimes and atmospheric processes into air quality assessments and environmental policy.

Supplementary Materials: The following supporting information can be downloaded at https://www.mdpi.com/article/10.3390/atmos17040399/s1, Figure S1. Schematic representation of a boxplot illustrating the main statistical components of the data distribution. The box represents the interquartile range (IQR), bounded by the first (Q1) and third quartiles (Q3), while the horizontal line inside the box indicates the median. Whiskers extend to the minimum and maximum values within 1.5 × IQR, and values beyond this range are classified as outliers (red circles). Table S1. AQI categories and corresponding $PM_{2.5}$ breakpoints (adopted by CONAMA, 2024 [34]). Figure S2. Time series of the AQI calculated using bias-corrected $PM_{2.5}$ concentrations from MERRA-2 (1980–2024) and CONAMA (2024) categories.

Author Contributions: Conceptualization, R.P., A.M., R.d.C.F., F.G.M., M.A.F. and D.N.; Methodology, R.P., A.M., D.N., F.O., G.C., B.I. and J.d.A.S.J.; Validation, R.P., D.N., A.M. and M.M.: Software; R.P.,

M.A.F., F.O., M.B. and F.G.M.; Formal analysis, R.P., D.N., A.M., L.F.A.C., F.G.M., M.A.F., T.R.R. and J.C.; Investigation, R.P., F.G.M., G.C., D.N., A.M., A.d.S., M.B. and R.d.C.F.; Resources, R.P., D.N., A.M., L.F.A.C., F.G.M., M.A.F., T.R.R., J.B. and J.C.; Data curation, R.P., A.M., D.N., F.O., G.C., B.I. and A.d.S.; Writing—original draft preparation; R.P., D.N., M.B., A.M., F.G.M., J.B. and M.A.F.; Supervision, R.P., D.N., F.G.M. and M.A.F.; Writing—review and editing; R.P. and D.N.; Project administration, R.P. All authors have read and agreed to the published version of the manuscript.

Funding: This research received no external funding.

Institutional Review Board Statement: Not applicable.

Informed Consent Statement: Not applicable.

Data Availability Statement: The raw data supporting the conclusions of this article will be made available by the authors on request.

Acknowledgments: The Postgraduate Program in Environmental Physics (PPGFA) of the Federal University of Mato Grosso (UFMT) and to the Meteorological Computing Laboratory of the Faculty of Meteorology (LACOMET) of the Federal University of Pará (UFPA). R.C.F. acknowledges the Conselho Nacional de Pesquisa e Desenvolvimento Científico—CNPq, project number 302248/2024-2. M.A.F. acknowledges the Conselho Nacional de Desenvolvimento Científico e Tecnológico—CNPq, project number 407752/2023-4.

Conflicts of Interest: The authors declare no conflicts of interest.

References

1. United Nations. Sustainable Development Goals. Climate Action, News, Press Material. United Nations Announces 2019 Climate Action Summit 'Clean Air Initiative', Calls on Governments at All Levels to Join. 2019. Available online: https://www.un.org/sustainabledevelopment/blog/2019/07/clean-air--initiative-calls-climate-action/ (accessed on 1 May 2025).
2. Vos, T.; Lim, S.S.; Abbafati, C.; Abbas, K.M.; Abbasi, M.; Abbasifard, M.; Abbasi-Kangevari, M.; Abbastabar, H.; Abd-Allah, F.; Abdelalim, A.; et al. Global burden of 369 diseases and injuries in 204 countries and territories, 1990–2019: A systematic analysis for the Global Burden of Disease Study 2019. *Lancet* **2020**, *396*, 1204–1222. [CrossRef]
3. WHO. The News from World Health Organization (WHO). 2020. Available online: https://www.who.int/health-topics/air-pollution/ (accessed on 1 May 2025).
4. Yu, W.; Guo, Y.; Shi, L.; Li, S. The association between long-term exposure to low-level PM2.5 and mortality in the state of Queensland, Australia: A modelling study with the difference-in-differences approach. *PLoS Med.* **2020**, *6*, 1003141. [CrossRef]
5. Miranda, R.M.; Andrade, M.F.; Fornaro, A.; Astolfo, R.; de Andre, P.A.; Saldiva, P. Urban air pollution: A representative survey of PM 2.5 mass concentrations in six Brazilian cities. *Air Qual. Atmos. Health* **2012**, *5*, 63–77. [CrossRef]
6. Fernandes, M.A.O.; Andreão, W.L.; Maciel, F.M.; Albuquerque, T.T.A. Avoiding hospital admissions for respiratory system diseases by complying to the final Brazilian air quality standard: An estimate for Brazilian southeast capitals. *Environ. Sci. Pollut. Res.* **2020**, *27*, 35889–35907. [CrossRef]
7. Requia, W.J.; Amini, H.; Mukherjee, R.; Gold, D.R.; Schwartz, J.D. Health impacts of wild fi re-related air pollution in Brazil: A nationwide study of more than 2 million hospital admissions between 2008 and 2018. *Nat. Commun.* **2021**, *12*, 6555. [CrossRef]
8. Franco, M.A.; Morais, F.G.; Rizzo, L.V.; Palácios, R.; Valiati, R.; Teixeira, M.; Machado, L.A.; Artaxo, P. Aerosol optical depth and water vapor variability assessed through autocorrelation analysis. *Meteorol. Atmos. Phys.* **2024**, *136*, 15. [CrossRef]
9. Nassarden, D.; Menezes, J.; Pessoa, C.B.; Carneiro, A.; dos Santos, L.O.F.; Cirino, G.; Imbiriba, B.; Sallo, F.; Curado, L.F.A.; Rodrigues, T.R.; et al. Evaluation and calibration of MERRA-2 and CAMS reanalysis for PM2.5 in a semi-urbanized area in the south of the Amazon. *Air Qual. Atmos. Health* **2025**, *18*, 1957–1972. [CrossRef]
10. Vormittag, E.M.P.A.A.; Cirqueira, S.S.R.; Neto, H.W.; Saldiva, P.H.S. Análise do monitoramento da qualidade do ar no Brasil. *Estud. Avançados* **2021**, *35*, 7–30. [CrossRef]
11. Oliveira, I.N.; Oliveira, B.F.A.; Silveira, I.H.; Machado, L.M.G.; Villardi, J.W.R.; Ignotti, E. Air pollution from forest burning as environmental risk for millions of inhabitants of the Brazilian Amazon: An exposure indicator for human health. *Cad. Saúde Pública* **2023**, *39*, e00131422. [CrossRef]
12. Yin, S. Spatiotemporal variation of PM2.5-related preterm birth in China and India during 1990–2019 and implications for emission controls. *Ecotoxicol. Environ. Saf.* **2023**, *249*, 114415. [CrossRef] [PubMed]

13. Wei, J.; Wang, J.; Li, Z.; Kondragunta, S.; Anenberg, S.; Wang, Y.; Zhang, H.; Diner, D.; Hand, J.; Lyapustin, A.; et al. Long-term mortality burden trends attributed to black carbon and PM 2.5 from wildfire emissions across the continental USA from 2000 to 2020: A deep learning modelling study. *Lancet Planet. Health* **2023**, *7*, e963–e975. [CrossRef]
14. Yu, W.; Ye, T.; Zhang, Y.; Xu, R.; Lei, Y.; Chen, Z.; Yang, Z.; Zhang, Y.; Song, J.; Yue, X.; et al. Global estimates of daily ambient fine particulate matter concentrations and unequal spatiotemporal distribution of population exposure: A machine learning modelling study. *Lancet Planet. Health* **2023**, *7*, e209–e218. [CrossRef]
15. Ali, M.A.; Bilal, M.; Wang, Y.; Nichol, J.E.; Mhawish, A.; Qiu, Z.; Leeuw, G.; Zhang, Y.; Zhan, Y.; Liao, K.; et al. Accuracy assessment of CAMS and MERRA-2 reanalysis PM2.5 and PM10 concentrations over China. *Atmos. Environ.* **2022**, *288*, 119297. [CrossRef]
16. Inness, A.; Ades, M.; Agustí-Panareda, A.; Barré, J.; Benedictow, A.; Blechschmidt, A.M.; Dominguez, J.J.; Engelen, R.; Eskes, H.; Flemming, J.; et al. The CAMS reanalysis of atmospheric composition. *Atmos. Chem. Phys.* **2019**, *19*, 3515–3556. [CrossRef]
17. Si, X.; Mengersen, K.; Ye, C.; Hu, W. Interactive effect of air pollutant and meteorological factors on seasonal influenza transmission, Shanghai, China. *Atmos. Environ.* **2024**, *318*, 120208. [CrossRef]
18. Randles, C.A.; da Silva, A.M.; Buchard, V.; Colarco, P.R.; Darmenov, A.; Govindaraju, R.; Smirnov, A.; Holben, B.; Ferrare, R.; Hair, J.; et al. The MERRA-2 aerosol reanalysis, 1980 onward. Part I: System description and data assimilation evaluation. *J. Clim.* **2017**, *30*, 6823–6850. [CrossRef]
19. Buchard, V.; da Silva, A.M.; Randles, C.A.; Colarco, P.; Ferrare, R.; Hair, J.; Hostetler, C.; Tackett, J.; Winker, D. Evaluation of the surface PM2.5 in version 1 of the NASA MERRA aerosol reanalysis over the United States. *Atmos. Environ.* **2016**, *125*, 100–111. [CrossRef]
20. Ouma, Y.O.; Keitsile, A.; Lottering, L.; Nkwae, B.; Odirile, P. Spatiotemporal empirical analysis of particulate matter PM2.5 pollution and air quality index (AQI) trends in Africa using MERRA-2 reanalysis datasets (1980–2021). *Sci. Total Environ.* **2024**, *912*, 169027. [CrossRef] [PubMed]
21. Li, L.; Qian, J.; Ou, C.-Q.; Zhou, Y.-X.; Guo, C.; Guo, Y. Spatial and temporal analysis of Air Pollution Index and its timescale-dependent relationship with meteorological factors in Guangzhou, China, 2001–2011. *Environ. Pollut.* **2014**, *190*, 75–81. [CrossRef] [PubMed]
22. Guo, J.; Xia, F.; Zhang, Y.; Liu, H.; Li, J.; Lou, M.; He, J.; Yan, Y.; Wang, F.; Min, M.; et al. Impact of diurnal variability and meteorological factors on the PM2.5-AOD relationship: Implications for PM2.5 remote sensing. *Environ. Pollut.* **2017**, *221*, 94–104. [CrossRef]
23. Zhou, Y.; Yue, Y.; Bai, Y.; Zhang, L. Effects of Rainfall on PM2.5 and PM10 in the Middle Reaches of the Yangtze River. *Adv. Meteorol.* **2020**, *2020*, 2398146. [CrossRef]
24. Li, X.; Feng, Y.J.; Liang, H.Y. The Impact of Meteorological Factors on PM2.5 Variations in Hong Kong. *Earth Environ. Sci.* **2017**, *78*, 012003. [CrossRef]
25. Gutierrez, C.B.B.; de Souza, E.B.; Gutierrez, D.M.G. Global/Regional Impacts on Present and Near-Future Climate Regimes in the Metropolitan Region of Belém, Eastern Amazon. *Atmosphere* **2022**, *13*, 1077. [CrossRef]
26. Furtado, L.S.; Pereira, R.V.S.; de Souza, E.B. Hemeroby Mapping of the Belém Landscape in Eastern Amazon and Impact Study of Urbanization on the Local Climate. *Urban Sci.* **2024**, *8*, 15. [CrossRef]
27. IBGE. Instituto Brasileiro de Geografia e Estatística. 2022. Available online: https://www.ibge.gov.br/cidades-e-estados/am/.html/ (accessed on 9 May 2025).
28. Souza, E.B.; Ferreira, D.B.d.S.; Santos, A.P.P. Observational Evidence of Intensified Extreme Seasonal Climate Events in a Conurbation Area Within the Eastern Amazon. *Earth* **2025**, *6*, 112. [CrossRef]
29. Chin, M.; Diehl, T.; Tan, Q.; Prospero, J.M.; Kahn, R.A.; Remer, L.A.; Yu, H.; Sayer, A.M.; Bian, H.; Geogdzhayev, I.V.; et al. Multi-decadal aerosol variations from 1980 to 2009: A perspective from observations and a global model. *Atmos. Chem. Phys.* **2014**, *14*, 3657–3690. [CrossRef]
30. Ukhov, A.; Mostamandi, S.; Silva, A.; Flemming, J.; Alshehri, Y.; Shevchenko, I.; Stenchikov, G. Assessment of natural and anthropogenic aerosol air pollution in the Middle East using MERRA-2, CAMS data assimilation products, and high-resolution WRF-Chem model simulations. *Atmos. Chem. Phys.* **2022**, *20*, 9281–9310. [CrossRef]
31. Said, S.; Salah, Z.; Hassan, I.A.; Wahab, M.M.A. COVID-19 Lockdown: Impact on PM10 and PM2.5 in Six Megacities in the World Assessed Using NASA's MERRA-2 Reanalysis. *Asian J. Atmos. Environ.* **2022**, *16*, 2021146. [CrossRef]
32. Provençal, S.; Buchard, V.; da Silva, A.M.; Leduc, R. Evaluation of PM surface concentrations simulated by Version 1 of NASA's MERRA Aerosol Reanalysis over Europe. *Atmos. Pollut. Res.* **2017**, *8*, 374–382. [CrossRef] [PubMed]
33. Navinya, C.D.; Vinoj, V.; Pandey, S.K. Evaluation of PM2.5 Surface Concentrations Simulated by NASA's MERRA Version 2 Aerosol Reanalysis over India and its relation to the Air Quality Index. *Aerosol Air Qual. Res.* **2020**, *20*, 1329–1339. [CrossRef]
34. CONAMA, Conselho Nacional de Meio Ambiente. Resolução nº 506, de 5 de Julho de 2024. 2024. Available online: https://conama.mma.gov.br/ (accessed on 10 May 2025).

35. McKee, T.B.; Doesken, N.J.; Kleist, J. The relationship of drought frequency and duration to time scales. In *Proceedings of the 8th Conference on Applied Climatology, Anaheim, CA, USA, 17–22 January 1993*; American Meteorological Society: Anaheim, CA, USA, 1993; pp. 179–184.
36. Satyamurty, P.; de Castro, A.A.; Tota, J.; Gularte, L.E.d.S.; Manzi, A.O. Rainfall trends in the Brazilian Amazon Basin in the past eight decades. *Theor. Appl. Climatol.* **2010**, *99*, 139–148. [CrossRef]
37. Curado, L.F.A.; de Paulo, S.R.; da Silva, H.J.A.; Palácios, R.S.; Marques, J.B.; de Paulo, I.J.C.; Dalmagro, H.J.; Rodrigues, T.R. Effect of biomass burning emission on carbon assimilation over Brazilian Pantanal. *Theor. Appl. Climatol.* **2023**, *155*, 999–1006. [CrossRef]
38. WHO, World Health Organization. WHO Global Air Quality Guidelines. 2021. Available online: https://iris.who.int/server/api/core/bitstreams/551b515e-2a32-4e1a-a58c-cdaecd395b19/content/ (accessed on 10 May 2025).
39. Almeida, G.P.; Bittencourt, A.T.; Evangelista, M.S.; Vieira-Filho, M.S.; Fornaro, A. Characterization of aerosol chemical composition from urban pollution in Brazil and its possible impacts on the aerosol hygroscopicity and size distribution. *Atmos. Environ.* **2019**, *202*, 149–159. [CrossRef]
40. Yousefi, R.; Shaheen, A.; Wang, F.; Ge, Q.; Wu, R.; Lelieveld, J.; Wang, J.; Su, X. Fine particulate matter (PM2.5) trends from land surface changes and air pollution policies in China during 1980–2020. *J. Environ. Manag.* **2023**, *326*, 116847. [CrossRef] [PubMed]
41. Omokpariola, D.O. Spatiotemporal analysis of atmospheric aerosols in African environments using MERRA-2 data (1980–2024): Impacts on climate extremes. *iScience* **2025**, *28*, 112995. [CrossRef]
42. Costa, L.R.R.; Ferreira, D.B.d.S.; Senna, R.C.; de Sousa, A.M.L.; Carmo, A.M.C.d.; Silva, J.d.A., Jr.; de Souza, F.G.; de Souza, E.B. River Stage Variability and Extremes in the Itacaiúnas Basin in the Eastern Amazon: Machine Learning-Based Modeling. *Hydrology* **2025**, *12*, 115. [CrossRef]
43. Neto, A.V.N.; de Souza, E.B.; Vasconcellos, F.C.; Ferreira, D.S.; Franco, V.S.; da Costa, C.P.W.; Jesus, E.S.; Tedeschi, R.G. Austral Autumn Precipitation Anomalies Across the Amazon Basin Under the Combined Influences of the Equatorial Pacific and Tropical Atlantic. *Int. J. Climatol.* **2025**, *45*, e8936. [CrossRef]
44. Rodrigues, S.; Cirino, G.; Moreira, D.; Pozzer, A.; Palácios, R.; Lee, S.C.; Imbiriba, B.; Nogueira, J.; Vitorino, M.I.; Vourlitis, G. Enhanced net CO_2 exchange of a semideciduous forest in the southern Amazon due to diffuse radiation from biomass burning. *Biogeosciences* **2024**, *21*, 843–868. [CrossRef]
45. Faria, A.L.S.; Freitas, R.A.P.; Souza, R.B.; Wallner-Kersanach, M.; Evangelista, H.; Moura, R.; Contreira-Pereira, L.; Mirlean, N.; Seus-Arrache, E.R.; Machado, E.C. The Role of the Intertropical Convergence Zone on the Aerosol Transport Pathways from Africa Towards the Western Tropical Atlantic Ocean. *Int. J. Climatol.* **2025**, *45*, e8910. [CrossRef]
46. Gutleben, M.; Groß, S.; Heske, C.; Wirth, M. Wintertime Saharan dust transport towards the Caribbean: An airborne lidar case study during EUREC4A. *Atmos. Chem. Phys.* **2022**, *22*, 7319–7330. [CrossRef]
47. Won, W.S.; Oh, R.; Lee, W.; Ku, S.; Su, P.C.; Yoon, Y.J. Hygroscopic properties of particulate matter and effects of their interactions with weather on visibility. *Sci. Rep.* **2021**, *11*, 16401. [CrossRef] [PubMed]
48. Andrade, M.F.; Kumar, P.; Freitas, E.D.; Ynoue, R.Y.; Jorge Martins, J.; Martins, L.D.; Nogueira, T.; Perez-Martinez, P.; Miranda, R.M.; Albuquerque, T.; et al. Air quality in the megacity of São Paulo: Evolution over the last 30 years and future perspectives. *Atmos. Environ.* **2017**, *159*, 66–82. [CrossRef]
49. Prospero, J.M.; Barkley, A.E.; Gaston, C.J.; Gatineau, A.; Campos y Sansano, A.; Panechou, K. Characterizing and quantifying African dust transport and deposition to South America: Implications for the phosphorus budget in the Amazon Basin. *Glob. Biogeochem. Cycles* **2020**, *34*, e2020GB006536. [CrossRef]
50. Urrutia-Pereira, M.; Rizzo, L.V.; Staffeld, P.L.; Chong-Neto, J.H.; Viegi, G.; Solé, D. Dust from the Sahara to the American Continent: Health impacts. *Allergol. Immunopathol.* **2021**, *49*, 187–194. [CrossRef] [PubMed]